Modeling Canopy CO2 Exchange in the European Russian Arctic

Authors: Kiepe, Isabell, Friborg, Thomas, Herbst, Mathias, Johansson, Torbjörn, and Soegaard, Henrik

Source: Arctic, Antarctic, and Alpine Research, 45(1) : 50-63

Published By: Institute of Arctic and Alpine Research (INSTAAR), University of Colorado

URL: https://doi.org/10.1657/1938-4246-45.1.50

Arctic, Antarctic, and Alpine Research, Vol. 45, No. 1, 2013, pp. 50–63

Modeling Canopy CO_2 Exchange in the European Russian Arctic

Isabell Kiepe‡*
*Thomas Friborg**
Mathias Herbst†
*Torbjörn Johansson** *and*
*Henrik Soegaard**

*Department of Geography & Geology, University of Copenhagen, Oester Voldgade 10, Copenhagen, 1350, Denmark
†Department of Bioclimatology, Göttingen University, Büsgenweg 2, Göttingen, Lower Saxony 37077, Germany
‡Corresponding author: ikiepe@yahoo.de

Abstract

In this study, we use the coupled photosynthesis-stomatal conductance model of Collatz et al. (1991) to simulate the current canopy carbon dioxide exchange of a heterogeneous tundra ecosystem in European Russia. For the parameterization, we used data obtained from *in situ* leaf level measurements in combination with meteorological data from 2008. The modeled CO_2 fluxes were compared with net ecosystem exchange (*NEE*), measured by the eddy covariance technique during the snow-free period in 2008.

The findings from this study indicated that the main state parameters of the exchange processes were leaf area index (*LAI*) and Rubisco capacity (V_{cmax}). Furthermore, this ecosystem was found to be functioning close to its optimum temperature regarding carbon accumulation rates. During the modeling period from May to October, the net assimilation was greater than the respiration, leading to a net accumulation of 58 g C m^{-2}. The model results suggest that the tundra ecosystem could change from a carbon sink to a carbon source with a temperature rise of only 2–3 °C. This is due to the fact that, in the continental Arctic, a global warming of a few degrees might restrict the net assimilation, due to high temperatures, whereas the respiration is predicted to be enhanced. However, future changes in vegetation composition and growth, along with acclimation to the new thermal regime, might facilitate the assimilation to counterbalance the carbon losses.

DOI: http://dx.doi.org/10.1657/1938-4246-45.1.50

Introduction

Terrestrial ecosystems in the Arctic play an important role in the global carbon cycle, because they contain at least one-third of the global terrestrial carbon, whilst covering 25% of the global land area (McGuire et al., 2009; Tarnocai et al., 2009). This region is predicted to undergo considerable future climate change, which might alter the net carbon exchange between the land and the atmosphere (IPCC, 2007; Qian et al., 2010).

To make predictions about the future net carbon exchange, it is necessary, however, to assess the present-day fluxes in terms of their controlling mechanisms. Successful modeling of net ecosystem carbon dioxide exchange in the Arctic relies on good estimates of the two major fluxes: carbon assimilation and ecosystem respiration. One challenge for modeling the carbon exchange on a regional scale is that the arctic landscape is a patchwork of differing plant species compositions, microtopography, water-table depth, and soil properties (Bliss and Matveyeva, 1992). Within the global network of micrometeorological flux measurements (FLUXNET), numerous ecosystem studies have been conducted in the boreal and temperate regions (Baldocchi et al., 2001), whereas detailed information about the dominant processes in the arctic region is comparably scarce.

Still, a number of models have been applied on a plot, landscape, or even regional scale to simulate the present-day carbon exchange in the Arctic. They vary in complexity, ranging from empirical models describing responses to environmental factors (e.g. Williams et al., 2006) to complex mechanistic or process-based models (e.g. *Ecosys*; Grant et al., 2003) (Fig. 1).

Empirical models use the combined representation of photosynthetic irradiance-response and temperature-sensitive respiration to scale carbon exchange from plot to landscape scale (e.g., Fox et al., 2008; Vourlitis et al., 2000), or for the interannual or regional comparison of the exchange (e.g., Lafleur and Humphreys, 2008; Laurila et al., 2001).

These regression-based models can be expanded to a regional scale through the use of multiple observations. Using such an empirical regression-based model, Zamolodchikov and Karelin (2001) simulated the carbon fluxes for the whole Russian tundra by evaluating the relation of the gross primary production to light, temperature, and seasonal phytomass dynamics. Requiring seasonal recalibration, empirical models provide useful information for regional or interannual comparison and the productivity of specific species. However, they are not intended for evaluating future responses of carbon budgets to changing climates, because the temperature response of photosynthesis is not taken into account.

The mechanistic and process-based models, on the other hand, include the temperature dependence of the processes involved, and are therefore suited to predicting future carbon exchange. These models attempt to represent specific interacting ecological process dynamics using a more detailed set of environmental and physiological parameters.

A mechanistic model developed by Farquhar et al. (1980) and further elaborated by Collatz et al. (1991) simulates the gas exchange of a canopy in free air using the big-leaf approach. This model, hereafter called the Collatz model, couples the modeling of net photosynthesis from environmental and leaf physiological parameters with a stomatal conductance model.

When extrapolating canopy models to landscape levels, a detailed knowledge of soil properties and hydrological conditions is required. This was demonstrated by models such as the soil-plant-atmosphere (SPA) continuum (Williams et al., 1996; Jarvis and

1523-0430/6 $7.00

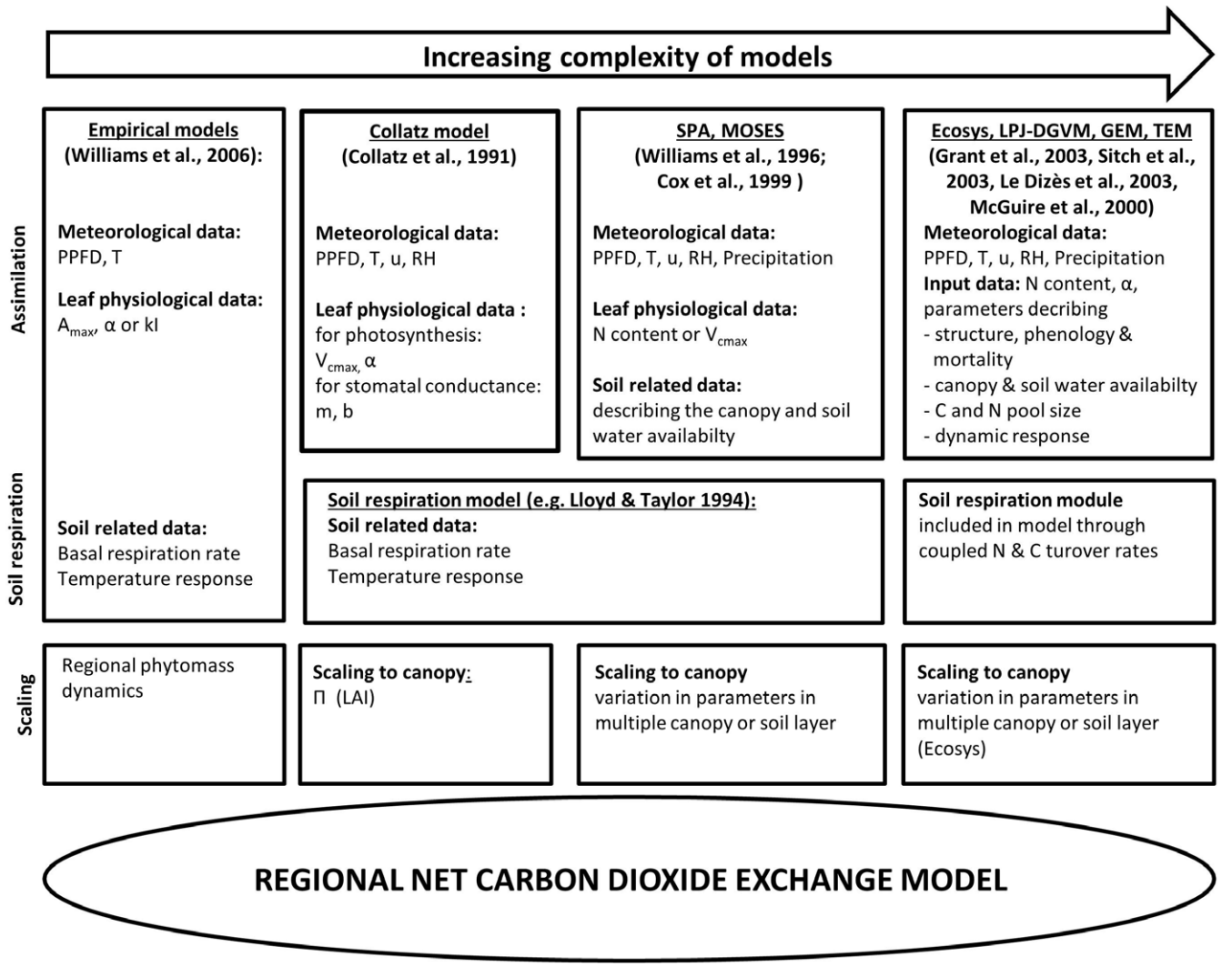

FIGURE 1. Schematic overview of different models and the main input parameters used in the Arctic.

McNaughton, 1986) and the Met Office Surface Exchange Scheme (MOSES) (Cox et al., 1999), which include the canopy and soil water availability for modeling the carbon assimilation rate. These models use the multilayer approach, separating the canopy and soil into several layers exhibiting different properties. Rennermalm et al. (2005) used MOSES to model the net carbon exchange in a high arctic site in Greenland using a four soil layer approach, while Williams et al. (2000) successfully tested the SPA model in northern Alaska using a two-layer canopy approach. Other process-based models (right-hand column in Fig. 1) have been applied for regional Pan-Arctic estimates of present and future carbon exchange processes, and these demand even more input parameters.

As only limited knowledge about soil and hydrological conditions in Northeast European Russia is available at present, in this study we evaluate the canopy carbon dioxide exchange in combination with estimates of soil respiration derived from the generalized temperature function described by Lloyd and Taylor (1994). This study focuses on the snow-free period from mid-May to the beginning of October. We recognize the importance of wintertime fluxes, because they can be substantial (Fahnestock et al., 1999; Bjorkman et al., 2010), but wintertime fluxes in remote areas can be hard to quantify. Therefore, the study period is restricted to the interval from early spring until late autumn.

We parameterized and tested the Collatz model for simulating the present-day net assimilation rate in the European Russian tundra, which covers an area of 232,000 km^2 (Zamolodchikov and Karelin, 2001). For the parameterization, site-specific input parameters are required. One important input parameter is Rubisco capacity (V_{cmax}). This study benefits from the fact that the V_{cmax} value was measured *in situ* on the representative plant species. The modeled CO_2 fluxes were compared to net ecosystem exchange (*NEE*) measurements obtained using the eddy covariance technique. We aim to identify the controlling parameters of net assimilation and to develop a tool for upscaling the results to a regional level. Furthermore, we attempt to analyze the temperature dependence in order to provide prospects for future carbon exchange mechanisms.

Material and Methods

SITE DESCRIPTION

This study was conducted in the discontinuous permafrost zone in the subarctic tundra of Komi Republic, Northeast European

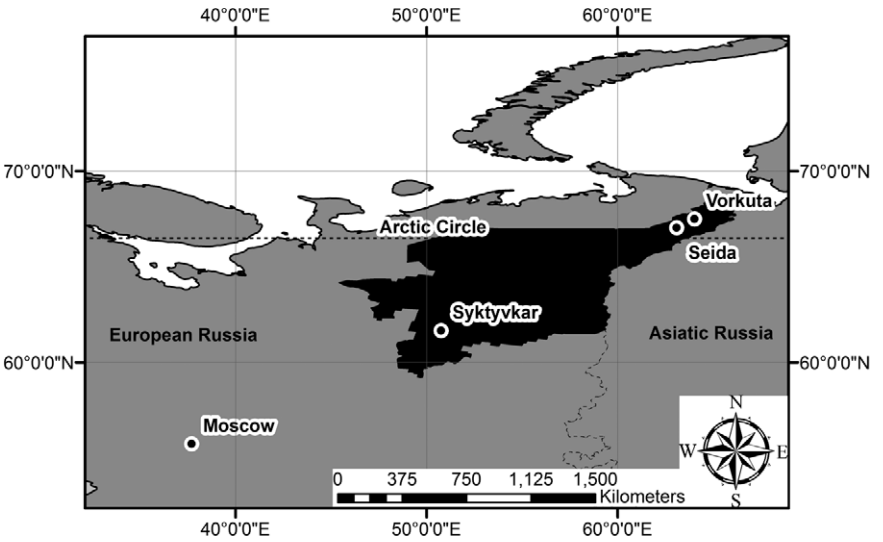

FIGURE 2. Location of Seida study site (67°03′N, 62°56′E) in the Komi Republic (black area), Russia.

Russia. The measurement site was located near the village Seida (67°03′N, 62°56′E, 100m a.s.l.) (Fig. 2).

Long-term average air temperatures for 1980–1999 from neighboring Vorkuta station (67°48′N, 64°01′E, 172 m a.s.l.) show a mean annual temperature in the region of −5.7 °C, with the coldest month being January (−20.1 °C) and the warmest July (12.8 °C). Long-term average precipitation records for 1980–1999 for Salekhard station (66°32′N, 66°36′E, 66 m a.s.l.) show an annual precipitation of 454 mm (data from Komi Republican Centre for Hydrometeorological and Environmental Monitoring).

The study site is a sedge-dwarf shrub tundra type, according to Bliss and Matveyeva (1992). Large parts of the landscape are shrub tundra dominated by *Betula nana*, *Salix* spp., and dwarf shrubs of heath species, *Empetrum nigrum*, *Ledum palustre*, and *Vaccinium* spp. (Table 1). The willow stands grow to a height of up to 1.5 m on low-lying parts of the landscape, which act as water drains in the partially frozen landscape. The remaining parts of the landscape are dominated by peat plateaus, thermokarst lakes, and narrow fens with high water tables, which surround the peat plateaus and thermokarst lake edges. The most characteristic vegetation in the fen is made up of *Carex* spp., *Eriophorum* spp., and mosses.

TABLE 1

Composition of land surface types with the dominant species in a 500 m radius around the measurement mast.

Land surface type	Dominant species	Area cover (%)
Tundra bog	*Sphagnum* ssp. *Ledum decumbens* *Empetrum hermaphroditum* (*nigrum*) *Rubus chamaemorus*	30
Tundra heath	*Ledum decumbens* *Empetrum hermaphroditum* *Vaccinium* ssp. (*vitis-idaea, uliginosum*) Mosses, reindeer lichens	26
Lakes		16
Fen	*Carex* ssp. *Sphagnum* ssp. *Salix* ssp. *Betula nana*	11
Betula nana heath	*Betula nana* (dominating)	9
Willows	*Salix* ssp. (i.e. *Salix lanata, phylicifolia, lapponum*)	3
Dry lichen tundra	*Ledum decumbens* *Empetrum hermaphroditum* *Vaccinium* ssp. (*vitis-idaea, uliginosum*) Lichens	3
Palsa	Bare peat (dominating)	1

COUPLED PHOTOSYNTHESIS–STOMATAL CONDUCTANCE MODEL

The Collatz model estimates the leaf gross photosynthesis rate (A_l) as the minimum process of three potential capacities, which are limited by different factors:

$$A_1 \approx \min \begin{Bmatrix} J_E \\ J_C \\ J_S \end{Bmatrix}. \quad (1)$$

J_E is the potential photosynthetic rate dependent on light:

$$J_E = a\alpha Q \frac{C_i - \Gamma_*}{C_i + 2\Gamma_*}, \quad (2)$$

where a is the absorptivity of the photosynthetic photon flux density (*PPFD*) for leaf material, α is the initial slope of the light response curve, Q is the *PPFD* in μmol m^{-2} s^{-1}, C_i is the internal CO_2 pressure in Pa and Γ_* is the compensation point in Pa.

J_C is the potential photosynthetic rate dependent on Rubisco capacity:

$$J_C = \frac{V_{cmax}(C_i - \Gamma_*)}{C_i + K_c\left(1 + \frac{O_2}{K_o}\right)}, \quad (3)$$

where V_{cmax} is the maximum catalytic capacity of Rubisco per leaf area unit in μmol m^{-2} s^{-1}, K_c and K_o are the Michaelis constant for CO_2 and the competitive inhibition constant for O_2 with respect to CO_2 in the Rubisco reaction.

J_S is the potential rate of export or utilization of the assimilated products and is proportional to the Rubisco capacity:

$$J_S = C_{Js} V_{cmax}, \quad (4)$$

where C_{Js} is a coefficient originally set to 0.5 (Collatz et al., 1991).

The temperature dependent parameters, i.e. τ, V_{cmax}, K_c, K_o, and R_{ld}, are scaled in accordance with Collatz et al. (1991) using the Q_{10} approach. The Q_{10} values were chosen according to Collatz et al. (1991), except the Q_{10} value for V_{cmax}, which was taken from Soegaard and Nordstroem (1999) and Cox et al. (1999) (Table 2).

In order to simulate realistic rates at high and low temperatures, a gradual temperature inhibition of V_{cmax} at high temperatures (s1) and of J_s at low temperatures (s2) is included (Alton and Bodin, 2010; Dang et al., 1998).

The dark respiration was calculated by:

$$R_{ld} = r V_{cmax}, \quad (5)$$

where r is a scaling factor derived from leaf level estimates of R_{ld} and V_{cmax} (see below).

The bulk stomatal conductance to water vapor per ground area unit (g_{sw}) is estimated using the Ball, Woodrow, and Berry model (BWB):

$$g_{sw} = m\frac{a_n h_s}{C_s} + b \quad (6)$$

where A_n is the net photosynthesis in mol m^{-2} s^{-1}, h_s is the relative humidity at the surface of the leaf, C_s is mole fraction of CO_2 at the surface of the leaf, and m and b are the slope and intercept of the BWB function, which can be obtained by linear regression analysis of data from gas exchange studies (Ball et al., 1987; Collatz et al., 1991).

A complete parameter list, including their temperature dependence, is shown in Table 2.

The photosynthesis rate of the upper sunlit leaves (A_l) is scaled to the canopy (A_n) using a canopy factor:

$$A_n = A_l \Pi - R_{ld} \Pi, \quad (7)$$

where A_l is the gross leaf photosynthesis rate, A_n is the net photosynthesis rate of the canopy, and R_{ld} is the dark respiration per unit leaf area, including the respiration that occurs during both day and night. Π is the canopy factor describing the area of sunlit leaves per ground area unit using Beer's law of light extinction (Sellers et al., 1992):

$$\Pi = \frac{(1 - e^{-kLAI})}{k} \quad (8)$$

where *LAI* is the leaf area index, and k is the extinction coefficient (Kull and Jarvis, 1995). The extinction coefficient relates to the solar elevation angle, β, by $k = 0.5/\sin\beta$ (Baldocchi, 1994). In this model, we only consider the sunlit leaves, as the number of shaded leaves is small due to the low *LAI*.

TABLE 2

Parameters and constants used in the model.

Parameter		Method/source	value	Q_{10}	unit
a	Absorptivity of PPFD	Collatz et al., 1991	0.86		(%)
K_c	Michaelis constant for carboxylation	Collatz et al., 1991	30	2.1	(Pa)
K_o	Michaelis constant for oxygenation	Collatz et al., 1991	30000	1.2	(Pa)
O_2	Partial pressure of oxygen	Collatz et al., 1991	20900		(Pa)
τ	Specific factor for Rubisco	Collatz et al., 1991	2600	0.57	(—)
s1	High temperature limitation of V_{cmax}	Alton and Bodin, 2010	40		(°)
α	Quantum use efficiency	initial slope of light response curve	0.07		(μmol CO_2 μmol photon^{-1})
V_{cmax}	Rubisco capacity at 25 °C	initial slope of A/C_i curve	45	2.0	(μmol m^{-2} s^{-1})
r	Scaling factor for R_{ld}	linear regression of R_{ld} vs. V_{cmax}	0.035	2.0	(%)
b	Intercept	linear regression in Figure 3	0.05		(mol m^{-2} s^{-1})
m	Slope	linear regression in Figure 3	6		(—)
C_{Js}	Scaling factor for export limitation	adjusted	1		(—)
s2	Cold limitation for export limitation	adjusted	0		(°C)

EDDY COVARIANCE MEASUREMENTS

For the validation of the model, the modeled canopy net assimilation rates are compared to the measured fluxes from the eddy covariance technique. The net ecosystem exchange (*NEE*) between the surface and the atmosphere was continuously measured using the micrometeorological eddy covariance method (Aubinet et al., 2000; Baldocchi, 2003). The system was set up with an R3 ultrasonic anemometer (Gill Instruments, U.K.) and an LI-7500 open-path (OP) CO_2/H_2O infrared gas analyzer (IRGA) (LI-COR Inc., U.S.A.) mounted at 3.95 m height on an extendable mast. The OP analyzer was tilted in a northern direction to minimize water coverage of the lower lens during rain events. Measurements were taken at a frequency of 10 Hz from 18 May until 6 October 2008. The raw data were processed using Alteddy software (version 3.5, Alterra, University of Wageningen, The Netherlands; http://www.climatexchange.nl/projects/alteddy/), which is based on EUROFLUX methodology discussed in Aubinet et al. (2000). The correction for artificial heating of the open-path system, as proposed by Burba et al. (2008), was included in the calculation of the half-hourly *NEE*. A detailed description of the data processing and footprint modeling is given in Marushchak et al. (2012).

The net assimilation rate (A_{nEC}) was estimated as:

$$A_{nEC} = NEP + R_{soil} \tag{9}$$

$$R_{soil} = R_{ECO} - R_d, \tag{10}$$

where *NEP* is the net ecosystem production, which equals the negative *NEE*, as measured by the eddy covariance, R_{soil} is the soil respiration, R_{ECO} is the ecosystem respiration, determined during nighttime, and R_d is the modeled canopy dark respiration. The respiration rates (R_i) were calculated using an Arrhenius type of function elaborated by Lloyd and Taylor (1994):

$$R_i = R_{10,i}\, exp^{\left(308.6\left(\frac{1}{56} - \frac{1}{(T_s + 46)}\right)\right)} \tag{11}$$

where $R_{10,i}$ is the respiration rate at 10 °C, T_s is the soil temperature in °C at 5 cm, and i represents either ecosystem, soil, or dark respiration.

The R_{10} of the ecosystem respiration (R_{ECO}) was estimated from the nighttime fluxes measured by the eddy covariance as 2.7 μmol m^{-2} s^{-1}, as described in Marushchak et al. (2012). The area integrated R_{10} of the dark respiration (R_d) was estimated from the leaf level measurements as 0.5 μmol m^{-2} s^{-1} (see below). According to Equation (10), the R_{10} of the soil respiration (R_{soil}) was calculated as 2.7 μmol m^{-2} s^{-1} − 0.5 μmol m^{-2} s^{-1} = 2.2 μmol m^{-2} s^{-1}.

SUPPLEMENTARY MEASUREMENTS

The development of the green leaf area index (*LAI*) was monitored using an LAI-2000 (LI-COR, Lincoln, Nebraska, U.S.A.) during the peak growing season (July–August). This was supplemented by spectral reflectance measurements in the red (F_R) and near infrared (F_{NIR}) part of the spectrum using a 2-channel spectrometer (Skye Instruments Ltd, Powys, U.K.). Using regression analysis, it was possible to determine the slope ($c = 0.28$) and the offset ($r_0 = 1.5$) in Equation (12) and thereby also estimate the *LAI* outside the peak growing season, in accordance with Soegaard et al. (2000):

$$LAI = c\left(\frac{R_{FR}}{R_R} - r_0\right). \tag{12}$$

To be able to upscale the *LAI* to landscape level, the level-4 MODIS global Leaf Area Index product was used as 8-day composites during the period from 8 May to 29 September 2008, at 1-km resolution (MODIS land product, Oak Ridge National Laboratory Distributed Active Archive Center (ORNL DAAC, 2009).

The basic meteorological parameters were recorded at the study site for the duration of the whole measurement campaign in 2008 using a CR23X logger (Campbell Scientific, U.K.). The following parameters were measured at half-hour intervals: air temperature and relative humidity (Hygrometer MP100A, Rotronic, U.S.A.), soil heat flux (HFP01, Hukseflux Thermal Sensors, The Netherlands), net radiation (NR LITE, Kipp and Zonen, The Netherlands), photosynthetic photon flux density (*PPFD*) (LI-190, LI-COR, U.S.A.), precipitation (7852 Rain Collector II, Davis, U.S.A.) and wind speed (A100R, Vector Instruments, U.K.).

The leaf temperature was estimated as:

$$T_l = \frac{Hr_{abw}}{\rho c_p} + T_a, \tag{13}$$

where H is the sensible heat flux in W m^{-2} measured by the eddy covariance technique, ρ is the air density in kg m^{-3}, c_p is the specific heat for air at constant pressure (1005 J kg^{-1} K^{-1}), T_a is the air temperature in K, and r_{abw} is the total resistance to water vapor calculated according to Monteith and Unsworth (1990).

The photosynthetic response curves of net assimilation vs. light and internal CO_2 concentration (A/C_i) were measured by a portable photosynthesis system (LI-6400, LI-COR Inc., Lincoln, Nebraska, U.S.A.) (Table 2). V_{cmax} was estimated from the initial slope of the A/C_i curves (Harley et al., 1992) and scaled to common temperature (25 °C; Leuning, 1997).

Results

PARAMETERIZATION OF THE MODEL

The model requires a set of input parameters, which describe the leaf physiological parameters, such as Rubisco capacity (V_{cmax}), quantum use efficiency (α), and scaling factor for R_{ld} (r), leaf area index (*LAI*), and the meteorological conditions.

Leaf Physiological Input Parameters

For the description of the leaf physiological parameters, representative values for the study site were chosen from four measured species (*Salix lanata*, *Salix phylicifolia*, *Carex aquatilis*, and *Rubus chamaemorus*). The quantum use efficiency (α) was found to vary between 0.06 and 0.09 μmol CO_2 μmol $photon^{-1}$. This can be compared to the values of 0.07 μmol CO_2 μmol $photon^{-1}$ derived from the eddy covariance data. The scaling factor for R_{ld} (r) was estimated as 0.035 for the four species, which lies in a similar magnitude to that reported in other studies (Miao et al., 2009; Rodeghiero et al., 2007). The Rubisco capacity at 25 °C (V_{cmax25}) was found to range from 27 to 51 μmol m^{-2} s^{-1} among the four species. Taking the composition of the landscape into account, the

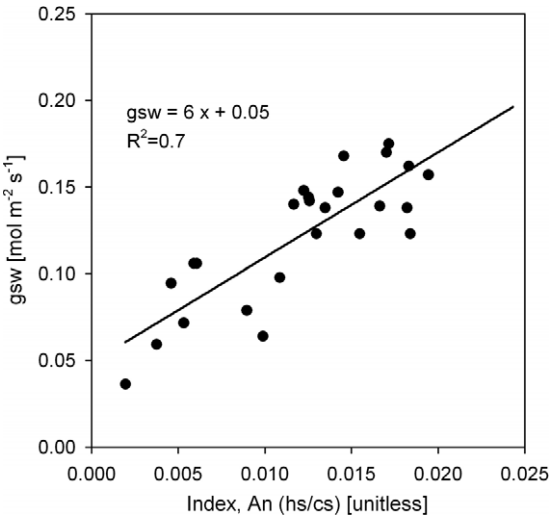

FIGURE 3. The slope (*m*) and intercept (*b*) of the response of stomatal conductance (*gsw*) to the index of the rate of net CO_2 uptake (A_n), the relative humidity (h_s) and the CO_2 mole fraction (C_s) of the air at the leaf surface are obtained by linear regression analysis of ambient measurements from gas exchange studies.

(dwarf) shrubs/willow (*Salix* spp.) were the representative vegetation type, because they are the most abundant species. Even if land-cover classes (willow and *Betula nana* heath) only cover 12% of the study site, the dwarf shrubs were found in most of the other land-cover classes. For this reason V_{cmax25}, representing the entire study area, was derived from two *Salix* species to 45 μmol m^{-2} s^{-1}.

The slope (*m*) and intercept (*b*) of the response of the stomatal conductance (g_{sw}) to the rate of net CO_2 uptake (A_n), relative humidity (h_s), and CO_2 mole fraction (C_s) of the air at the leaf surface were obtained from the leaf-level measurements [Equation (6)]. A linear regression analysis of the ambient measurement of the A/C_i curves is shown in Figure 3.

Leaf Area Index for Scaling from Leaf to Canopy

The MODIS *LAI* data were compared to the handheld *LAI* measurements, showing that values nearly doubled during the peak growing season. Additionally, we found that the satellite-derived *LAI* values also increased during early spring. The bud break of the deciduous shrubs was noted on 19 June. The re-greening of the evergreen dwarf shrubs was observed on 17 June. A similar increase of satellite-derived *LAI* prior to the bud break was made by Verbyla (2005) in Alaska, who attributed this artificial increase to the snowmelt. In accordance with this, the *LAI* increase was delayed until 17 June through extrapolation of the measured *LAI* by the spectrometer. The last snow patches disappeared on 25 June, so the recalibrated MODIS data were used after that date. By combining the three methods, the development of the green *LAI* during the growing season was derived (Fig. 4).

The daily midday extinction coefficient is around 0.7 until the end of July. After that, the extinction coefficient starts increasing, because the solar elevation angle decreases, leading to a longer path length through the canopy. The extinction coefficient continues to increase as the solar elevation angle decreases until it reaches a maximum value of 1.7 in the beginning of October. At that time, the sine of the solar elevation angle reaches half of its initial value in May, which equals a decrease from the maximum solar elevation angle of 46° in June to 17° in October. Comparable extinction coefficients were measured in arctic tundra ecosystems ranging from 0.9 during April and May in subarctic Canada (Bewley et al., 2007) and during July and August in a high arctic site in Greenland (Soegaard and Nordstroem, 1999) to 1.9 during July and August in a modeling study for tundra ecosystems (Shaver et al., 2007).

Meteorological and Radiation Input Parameters

The seasonal variation of the meteorological input parameters of air, soil, and leaf temperature; photosynthetic photon flux density (*PPFD*); and relative humidity is shown in Figure 5.

The measurements started on 18 May 2008 (DOY 139), when the half-hourly average air temperatures were mainly below 0 °C, and the landscape was partly covered in snow. The average soil temperatures at 2 cm depth remained negative until 27 May (DOY 148). After that, only nighttime soil temperatures reached 0 °C, while daytime soil temperatures approached 2–3 °C. From 10 June onwards, no negative soil temperatures were measured until 26 September (DOY 270). The daily temperature rose until the end of July, with a daily average maximum of 23 °C in the air and 24 °C at the leaf surface on 23 July (DOY 205). The soil temperatures in 5 cm depth reached a maximum value of 16 °C.

A maximum half-hourly *PPFD* value of 1300 μmol m^{-2} s^{-1} was measured at the middle of July. Low *PPFD* levels (<50 μmol m^{-2} s^{-1}) only occurred in May and June during the period from 9:30 p.m. to 3:00 a.m. local summer time, when the midnight sun occurred.

SEASONAL AND DIURNAL COURSE OF MODELED NET ASSIMILATION

The net assimilation (A_n) was modeled using the parameters listed in Table 2. The seasonal course of the modeled daily average

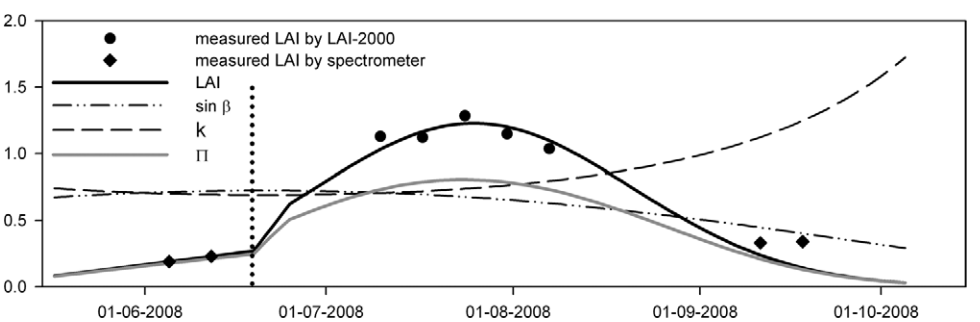

FIGURE 4. Development of measured and interpolated *LAI*, the sinus of the sun elevation (β), the extinction coefficient (k) and the canopy factor (Π) during the modeling period. The dotted line indicates the start of the bud break.

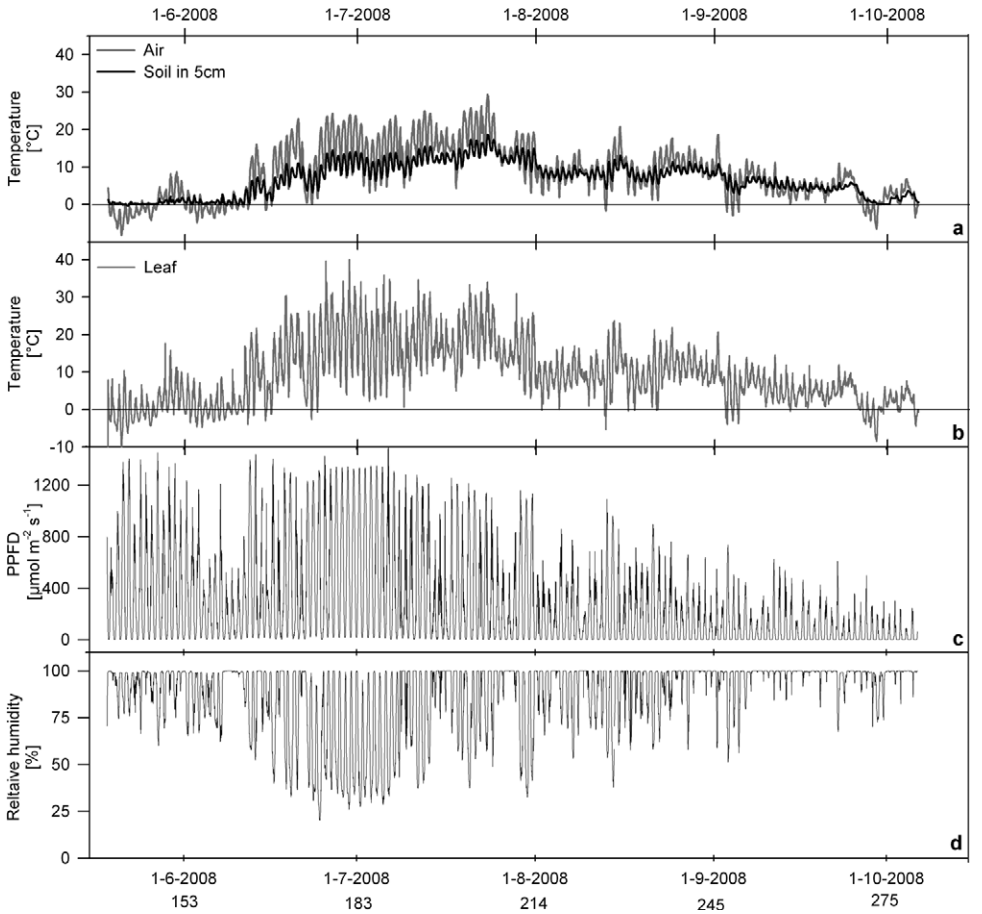

FIGURE 5. Seasonal course of selected meteorological parameters during the measurement campaign 2008: (a) air and soil temperature, (b) leaf temperature according to Equation (13), (c) photosynthetic photon flux density (*PPFD*), and (d) relative humidity.

A_n (black), the measured A_n as the sum of eddy covariance measurements (*NEP*) and the soil respiration (gray) are shown in Figure 6. The daily averages were calculated only from those half-hour intervals when an original flux from the eddy covariance data was available to avoid artificial error being possibly introduced by the gap-filling procedure.

The comparison of the modeled and measured fluxes showed an overall good agreement of the daily average fluxes during the growing season, as the values are scattered around the 1:1 line (gray line in Fig. 6 [right]). However, during early autumn, a difference between the modeled and measured fluxes was observed. By analyzing the diurnal course of the modeled A_n, we found that, especially during that period, the fluxes were often excessively limited by the export (J_s), leading to an underestimation of the modeled A_n compared to the measured A_n. For this reason, the scaling factor for export limitation (C_{Js}) was increased from 0.5 to 1. This modification weakened the influence of the limitation of the assimilation due to the removal of assimilates and thus increased the modeled A_n. A similar approach was taken in other northern latitude studies (Dang et al., 1998; Soegaard and Nordstroem, 1999). This change led to a decrease in root square mean error (RSME) from 1.68 $\mu mol\ m^{-2}\ s^{-1}$ to 1.49 $\mu mol\ m^{-2}\ s^{-1}$, because the underestimation in autumn decreased (Fig. 7). A statistical *t*-test demonstrated that the slope of the regression line with 0.9 differs significantly from 0, but not from the 1:1 line ($t = 4.3$).

Taking these aspects into account, the net carbon assimilation

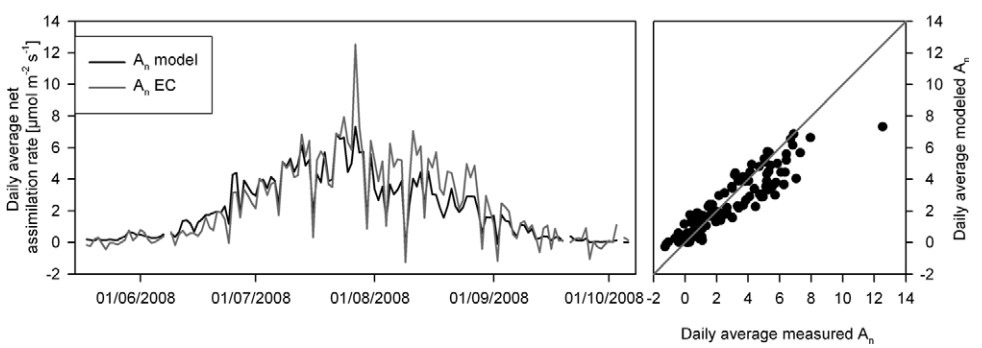

FIGURE 6. Daily average net assimilation rates derived from the Collatz model (black) and the original, not gap-filled fluxes measured by the eddy covariance technique, defined as $A_n\ EC = -NEE + R_{soil}$ (gray), (RSME = 1.68 $\mu mol\ m^{-2}\ s^{-1}$).

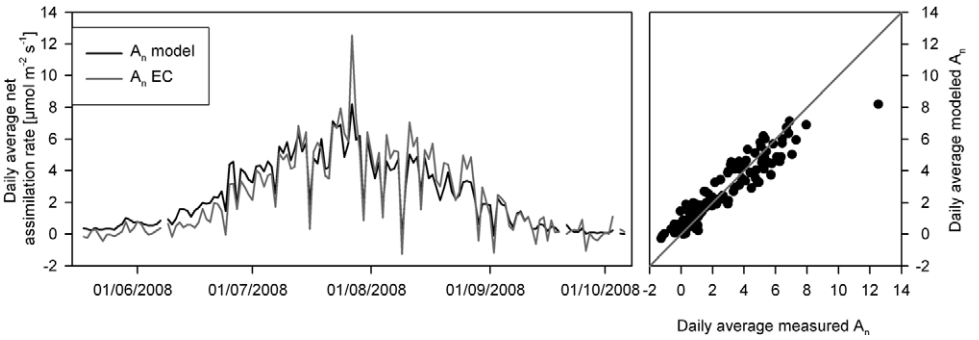

FIGURE 7. Daily average net assimilation rates derived from the Collatz model (black) and the original, not gap-filled fluxes measured by the eddy covariance technique, defined as $A_n\ EC = -NEE + R_{soil}$ (gray), including a change of C_{Js} from 0.5 to 1 (RSME = 1.49 µmol m^{-2} s^{-1}).

for a heterogeneous tundra ecosystem can be adequately simulated using the Collatz model. As shown in Figure 8, the modeled cumulative A_n amounts to 306 g C m^{-2} over the measurement period from mid-May to the beginning of October. The measured cumulative A_n is 31 g C m^{-2} lower, with the largest deviation from the model during the start of the growing season, but both curves feature the same slope.

For further examination of the model, four evenly distributed days were chosen to demonstrate the diurnal course of the measured and modeled A_n. Figure 9 shows the fluxes together with the three limiting rates on 22 June, 23 July, 23 August, and 10 September 2008. It is evident that during nighttime, light was the limiting factor of the fluxes, whilst during daytime, Rubisco capacity gained in importance as the limiting factor. On 22 June, 23 July, and 10 September, the CO_2 fluxes were limited only by the Rubisco limited rate (J_C), whereas the fluxes on 23 August were limited by both Rubisco (J_C) and light (J_E). The weakening of the influence of the export limitation (J_S) restricted the flux only as a co-limitation, e.g., on 22 June in the morning.

A sensitivity test was conducted on the modeled half-hourly fluxes for the input parameters *LAI*, leaf temperature, and Rubisco capacity (V_{cmax}), while other parameters were unchanged and set to a *PPFD* of 1150 µmol m^{-2} s^{-1}, a relative humidity of 70%, and the extinction coefficient of 0.7 (Fig. 10). For all three parameters, A_n shows a distinct response. The V_{cmax} has the greatest potential for an increase in A_n, because A_n almost doubles when doubling the V_{cmax} to 90 µmol m^{-2} s^{-1}. A_n also almost doubles when *LAI* is increased from 0.5 to 1, but subsequently increases less with higher *LAI*. The temperature exerts a positive influence on the assimilation at first, but at high temperatures, above 30 °C, the modeled rates decrease due to the high-temperature constraints.

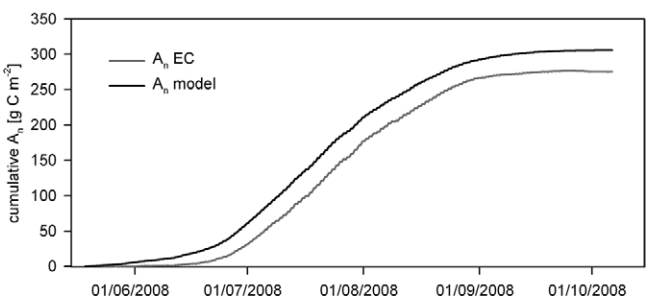

FIGURE 8. Modeled and measured cumulative net assimilation rates over the measurement period 2008. The estimated error of the model was found to be ±5.1 g C m^{-2} (Soegaard et al., 2000), while the estimated error of the measured flux data is ±49.8 g C m^{-2}, due to the uncertainty in the gapfilling procedure (Marushchak et al., 2012).

NET ECOSYSTEM CARBON DIOXIDE EXCHANGE IN THE CONTEXT OF CLIMATE CHANGE

For the evaluation of future carbon balance, the Collatz model was used for the simulation of A_n at variable air and soil temperatures and a higher atmospheric CO_2 concentration. The air and soil temperatures were changed in 2 °C intervals from 4 °C below to 6°C above 2008 levels, while the atmospheric CO_2 concentration was increased to a value of 470 ppm (according to the recent growth rates and concentrations from http://www.esrl.noaa.gov/gmd/ccgg/trends/). It was assumed that a temperature increase would affect the soil and air temperature equally. All other meteorological conditions, such as precipitation, radiation, and relative humidity, remained the same as in the year 2008. Only the length of the growing season was adjusted, as a temperature change results in a longer growing season. In order to estimate the prolongation, we calculated the growing season according to the sum of days exceeding 5 °C on five consecutive days. This temperature threshold was previously applied in the Arctic by Groendahl et al. (2007) and Aurela et al. (2001). By increasing the air temperature, the length of the growing season extended on average by 3 days per 1 °C temperature increase.

The model showed that this ecosystem accumulates 58.1 g C m^{-2} from mid-May to the beginning of October. The contributing fluxes include 305.6 g C m^{-2} net assimilation and 247.5 g C m^{-2} carbon loss through soil respiration. When soil and air temperatures rise, the Collatz model predicts that both net assimilation and soil respiration rates will increase (Fig. 11).

But as the soil respiration rates increase faster than the net assimilation rates, the carbon budget turns from sink to source, when temperatures rise more than 2 °C at current atmospheric CO_2 concentrations. The enhanced carbon loss is further facilitated as the simulated net assimilation rates cease to increase due to the high temperature inhibition of the photosynthesis. This restriction of the photosynthetic gains is important due to the relatively high summer temperatures experienced in continental arctic Russia.

Considering the present rate of increase in atmospheric CO_2, higher CO_2 concentrations are likely to accompany future temperature increases. When the ecosystem is not limited by nutrients (nitrogen or phosphorus), the CO_2 fertilization due to the higher CO_2 concentrations increases net assimilation rates, counteracting the enhanced losses due to the initial temperature increase. At higher CO_2 concentrations, the change from sink to source occurs beyond a temperature increase of 4 °C.

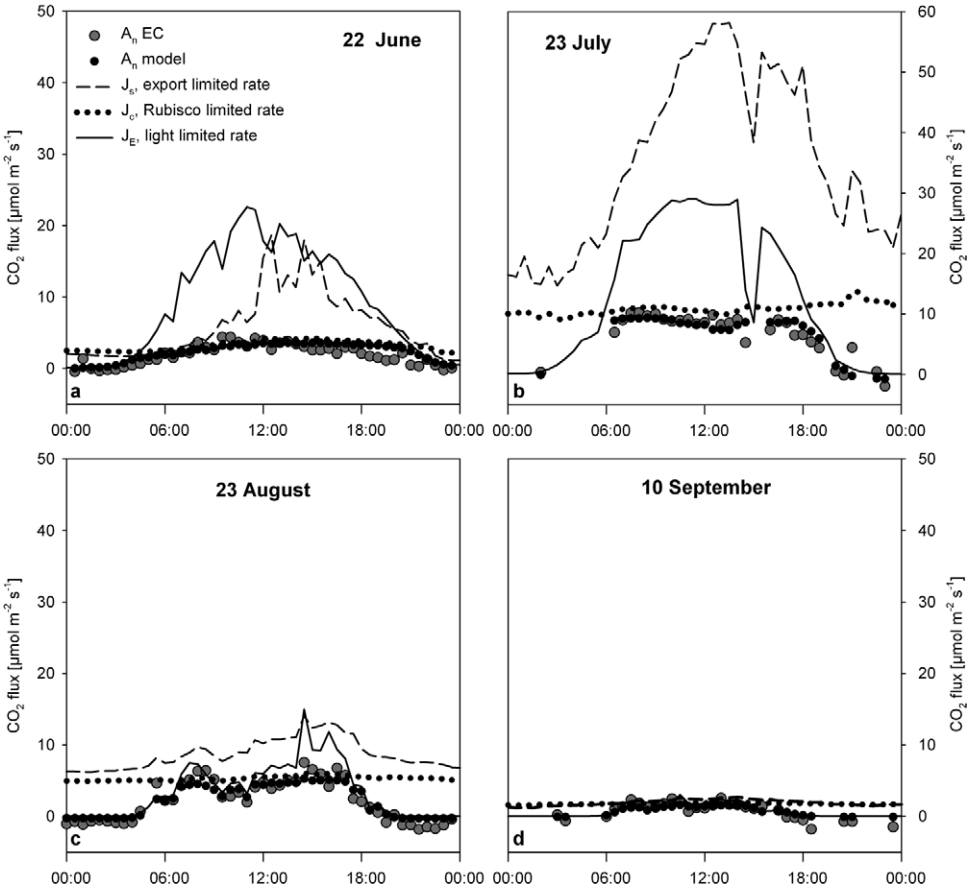

FIGURE 9. Four selected days illustrate the temporal variability of the net assimilation, including their three limiting rates during the growing season.

Discussion

MODELING THE NET ASSIMILATION RATE OF A HETEROGENEOUS TUNDRA

This study shows that the net carbon assimilation A_n amounted to 306 g C m^{-2} in Northeast European Russia over the measurement period from mid-May to the beginning of October 2008. When adding the modeled dark respiration (47g C m^{-2}) to A_n, the modeled gross primary production (*GPP*) amounted to 353g C m^{-2}. This carbon assimilation agrees with a *GPP* of 334.3 ± 41.3 g C m^{-2} estimated by Zamolodchikov and Karelin (2001) for the entire European Russian tundra. Also, other arctic studies measured *GPP* of a similar magnitude: approximately 310 g C m^{-2} were measured in a Canadian tundra by Nobrega and Grogan (2008) and 374 g C m^{-2} in a tussock tundra exhibiting extensive thaw in Alaska by Vogel et al. (2009).

The Collatz model was used in its standard setup with site-specific parameters (Table 2). The only necessary change was to weaken the export limitation, especially at cold temperatures, be-

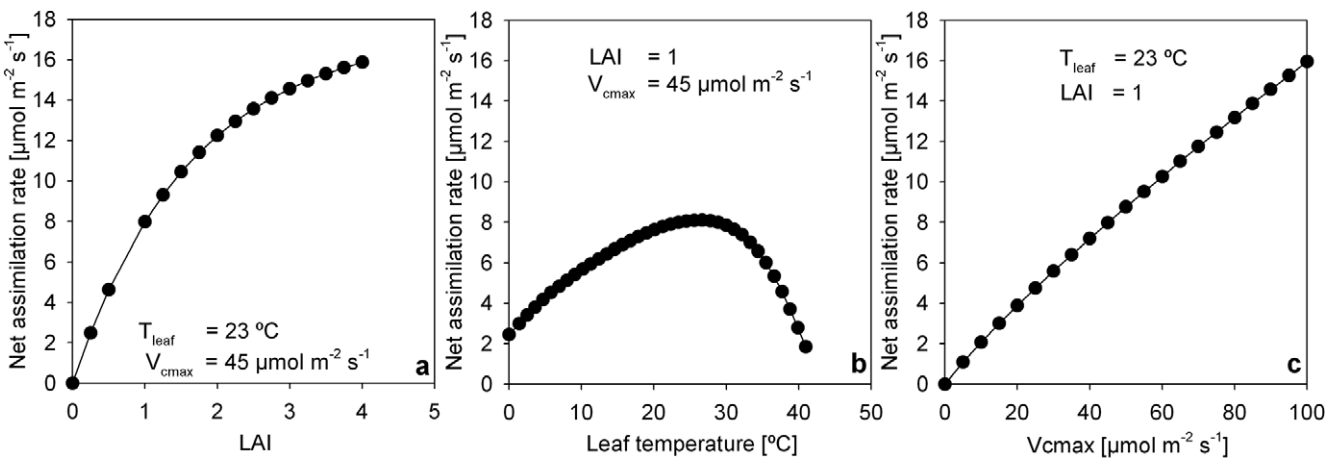

FIGURE 10. Results from a sensitivity test of the modeled half-hourly fluxes for the input parameters (a) *LAI*, (b) leaf temperature, and (c) Rubisco capacity, while other parameters were unchanged and set to measured values: 1150 µmol m^{-2} s^{-1} for *PPFD*, 70% for relative humidity, and 0.7 for the extinction coefficient.

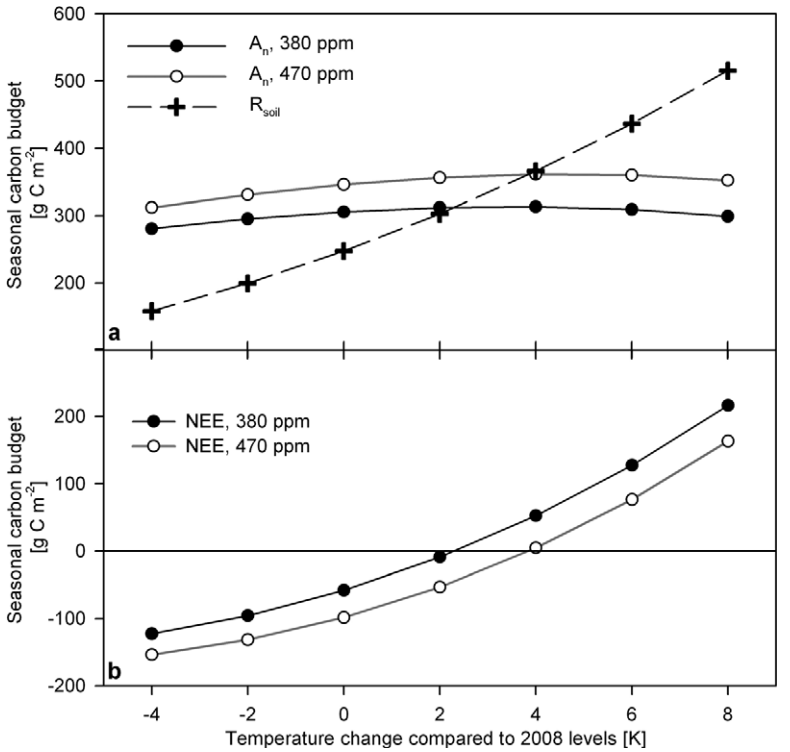

FIGURE 11. Carbon budget for the period from mid-May to beginning of October, with different temperatures and atmospheric CO_2 concentrations, separated into (a) net assimilation (A_n) and soil respiration (R_{soil}), and (b) combined to net ecosystem exchange (*NEE*).

cause we detected a systematic underestimation of the measured fluxes by this limitation. This might indicate that the translocation of the assimilates exerts a minor limitation, as demonstrated in models presented by Haxeltine and Prentice (1996) and Sitch et al. (2003). These models are able to simulate the assimilation rates considering only the light and Rubisco limitation processes.

The evaluation of the modeled fluxes also shows that the Rubisco capacity (V_{cmax}) is an important limiting factor for determining A_n. During the peak growing season, comprising July and August, 68% of the daytime fluxes were limited by the Rubisco capacity, whereas the remaining 32% were light limited. The influence of the export limitation was weakened, as discussed above, and thus exerted only marginal constraints. Consequently, V_{cmax} might have a significant influence on the magnitude of the net assimilation. Only sparse V_{cmax} data are available for arctic species. The V_{cmax25} of 45 μmol m^{-2} s^{-1}, determined in this study by leaf gas exchange measurements, is found to be of a similar magnitude as found in other arctic studies, as summarized in Table 3. Due to the wide range of values for Rubisco capacity, the representative value for the study area might be altered, affecting the net assimilation, when the composition of the plant species changes substantially.

Despite the good agreement between the modeled and measured daily values, there are discrepancies that reflect potential bias in the measurements and the model. The comparison shows that, during spring, the model overestimates the measured fluxes, accumulating to a difference of ca. 31 g C m^{-2}. The opposite was found in August, when the model underestimates the measured fluxes. These discrepancies can either be attributed to the measurements or the model, or a combination of both.

The model might introduce bias due to its parameterization, leading to the noted overestimation in spring and the underestimation in August. There are three possible reasons for the overestimation in spring. The biochemical parameters, such as V_{cmax}, might exhibit a seasonal course, starting with lower values during spring, increasing to larger values during peak growing season, and subsequently decreasing again. This seasonal pattern of V_{cmax} was found through inverse modeling in boreal forests (Thum et al., 2008) and might lead to an overestimation of the measured fluxes when using

TABLE 3

Overview of Rubisco capacity values in the Arctic.

V_{cmax} (μmol m^{-2} s^{-1})	V_{cmax25} at 25 °C (μmol m^{-2} s^{-1})	Site	Reference
	45	Willow, Russia	This study
17.8	62	Willow, Svalbard	Muraoka et al., 2002
18	50	Sedges, Greenland	Soegaard et al., 2000
21	60	Dwarf shrubs, Greenland	Soegaard et al., 2000
	50–86	Fen, Greenland	Rennermalm et al., 2005
7–131		Global scale	Wullschleger, 1993

a constant V_{cmax} value. Dang et al. (1998) demonstrated that a single mid-growing-season parameterization gave reasonable results, but the correlation coefficient was improved by including the seasonal variation. In this study, an introduction of a seasonal course would improve the model in the beginning of the growing season, but would increase the discrepancy in autumn by further reducing the modeled flux.

Another reason might be related to the estimation of the *LAI*. Using a combination of satellite data, spectrometer, and optical measurements, the *LAI* value reached $1.1-1.3$ during the peak growing season. Other studies in the Arctic have found *LAI* values similar to this study (Table 4). Compared to the *LAI*-2000 measurements, the MODIS-derived *LAI* was twice as high, which made a recalibration necessary.

Besides the peak value of the *LAI*, the start of the increase in *LAI*, in particular, governed A_n. Even if the meteorological conditions would allow photosynthesis in the model, the *LAI* has to be greater than 0 to simulate the carbon uptake at canopy level. However, during the start of the growing season, in particular, *LAI* estimates are challenging, because direct measurements using the *LAI*-2000 were not feasible, and the satellite-derived *LAI* might lead to an artificial increase due to snowmelt as shown by Verbyla (2005). This leads to an uncertainty of the timing of the vegetation growth, which might contribute to the earlier start of the modeled carbon assimilation compared to the measured values.

A third reason might be related to overestimation of soil respiration rates, resulting in larger measured net assimilation rates. Water saturated soil conditions in spring might limit the oxygen transport in the soil column and thus the aerobic decomposition (Hobbie et al., 2000). This might result in a lower actual soil respiration rate than the rate calculated from Equation (9), and thus lower measured A_n by the EC technique.

In contrast to the overestimation in spring, the model underestimates the measured fluxes in August in particular. The monthly average air temperature in August was 9 °C, with daily air temperatures ranging from 6 to 15 °C. This was significantly colder than July, with daily air temperatures ranging from 12 to 23 °C and a monthly average of 16 °C. The underestimation of the measured fluxes could be caused by the fact that the photosynthesis may not be as constrained at low temperatures as previously assumed. The original model setup includes a cold temperature inhibition in the export limitation (J_s). We already adapted this constraint by weakening the influence of J_s and lowering the cold inhibition temperature (s2) from 15 to 0 °C. This improved the model by decreasing the RSME from 1.68 μmol m^{-2} s^{-1} to 1.49 μmol m^{-2} s^{-1}, but did not fully solve the discrepancy. A similar observation was made by Williams et al. (2000). They were also able to improve the model by adjusting the low temperature inhibition to the extent that the photosynthetic rates were kept at 95% of their maxima at 5 °C.

TABLE 4

Overview of leaf area index (*LAI*) values in the Arctic.

LAI	Site	Reference
1.1–1.3	Shrub tundra, NE European Russia	This study
0.8–0.9	Birch hummock, dry heath, Canada	Nobrega and Grogan, 2008
1.1	Fen, Greenland	Soegaard et al., 2000
0.7–1.8	Shrub tundra, Alaska	McFadden et al., 2003
1.4	Wet tussock grassland, Siberia	Corradi et al., 2005

CARBON BUDGET UNDER A CHANGING CLIMATE

The mean annual air temperature is likely to increase up to 7 °C in arctic Russia by the end of this century (ACIA, 2005). The simulations with increasing air and soil temperatures showed how fragile this ecosystem is and how changes in temperature can weaken the sink strength or even turn the ecosystem into a carbon source. Under present-day meteorological and leaf physiological conditions (Fig. 5), the net assimilation will still be enhanced when the air temperature increases by 2 °C. As the net assimilation operates close to its optimum temperature, the biological activity would become restricted with further temperature increases, which was demonstrated in the sensitivity test. Over a longer period a temperature increase could lead to a shift in optimum temperature, as plants are able to adapt to changes in growing temperature (Sage and Kubien, 2007). The ability of shifts in the optimum temperature on the ecosystem level was demonstrated for subtropical to boreal ecosystems and related to temperature acclimation of gross ecosystem production (*GEP*) (Niu et al. 2012). A higher acclimation potential due to a wider range of temperature variability was found in northern populations of trees relative to their southern counterparts (Ghannoum and Way, 2011). This thermal acclimation would delimit the high-temperature inhibition, enabling the net assimilation rates to counterbalance the respiratory losses even at higher temperatures.

Generally, experimental warming studies (e.g. Welker et al., 2004; Oberbauer et al., 2007) or model projections (e.g. Sitch et al., 2007; Qian et al., 2010) indicate a greater increase in net primary production or *GEP* than in R_{ECO} in the Arctic. The increase in *GEP* is mainly caused by an increase in green biomass (Marchand et al., 2004) and more favorable temperature conditions (Callaghan et al., 2004). The response of *GEP* to warming can also be related to a latitudinal gradient (Oberbauer et al., 2007). They found that the smallest response of *GEP* to warming was in the southern part with higher temperatures. Considering that our study site is also experiencing relatively high temperatures during the growing season (Fig. 5), it seems plausible that the response to warming is less pronounced than in studies in the High Arctic (e.g. Welker et al., 2004; Marchand et al., 2004).

Additionally, increasing temperatures will not only lead to a longer growing season, which is positively related to carbon uptake (Lund et al., 2010; Groendahl et al., 2007), but might also introduce vegetation changes (Elmendorf et al., 2012). Observations based on satellite data and photographs taken during the last few decades show that this change has already started in the transition zone between taiga and tundra. An increase in normalized difference vegetation index (*NDVI*), visible as a ''greening'' of the tundra, has been observed in the circumpolar Arctic (e.g., Sturm et al., 2001; Forbes et al., 2010, Myers-Smith et al., 2011) and attributed to the expansion or increase in the height of shrubs, or both these factors, manifested in a larger *LAI* (Walker et al., 2006; Raynolds et al., 2008). Even though this model does not include a dynamic response of the carbon exchange process to changes in carbon and nitrogen pools, the sensitivity test indicates the ecosystem's potential to assimilate carbon. When running the existing model with

double the *LAI* values, keeping all other parameters at present-day values, the net carbon uptake would increase from 306 g C m^{-2} to 477 g C m^{-2}.

The warming experiments and model projections (e.g. Sitch et al., 2007; Qian et al., 2010) agree that the R_{ECO} will increase with rising temperatures. This is primarily caused by the exponential temperature dependence (Lloyd and Taylor, 1994), but also through unlocking carbon stored from the permafrost (Schuur et al., 2009). The effect of warming is further influenced by changes in the hydrology. Drier sites reacted more than wet sites (Oberbauer et al., 2007). Thus, a great uncertainty remains regarding the future hydrological regime in the study area, which will determine the increase in R_{ECO}. Under present hydrological conditions, an increase of R_{ECO} is projected, which is not constrained by oxygen-limited conditions.

Thus, if all other conditions were stable, this ecosystem would turn from a sink into a source with only a small increase in temperature. However, due to the changes, e.g. in plant composition and stature and hydrology, the response will be more complex.

Conclusion

The great advantage of the Collatz model compared to the complex process-based model is the relatively simple parameterization (Table 2). This study showed that, despite being a heterogeneous ecosystem, the model was able to simulate the fluxes using a single parameter set. The leaf area index (*LAI*) and the Rubisco capacity (V_{cmax}) were identified as two important parameters for modeling carbon dioxide exchange on a canopy scale. It was also shown that a constant value of V_{cmax} was able to capture the variation in A_n during the growing season. Furthermore, V_{cmax} is found to be a robust measure (45–62 μmol m^{-2} s^{-1}) for arctic ecosystems (Table 3).

This study provides a tool for scaling carbon fluxes to a larger area, such as the European Russian tundra. The combination of a constant V_{cmax} and regional satellite-based *LAI* values facilitates the upscaling of carbon exchange to a regional scale, where care should be taken that the satellite data should be validated against ground truth data in order to avoid possible errors.

Furthermore, this study showed that European Russian tundra is close to its optimum temperature with regards to carbon accumulation rates. At present, the net assimilation is greater than the respiration, leading to a net accumulation of 58 g C m^{-2} during our model period from mid-May to the beginning of October. This net gain becomes even smaller when considering the cold season respiratory losses used to calculate an annual budget. With increasing temperatures, the photosynthesis is predicted to become restricted by the high temperatures, exerting a strong limitation on the carbon uptake if no long-term acclimation occurs. The respiration, on the other hand, is predicted to be enhanced with increasing temperatures. Under these conditions, the European Russian tundra might turn into a net carbon source with rising temperatures. However, future changes in vegetation composition and growth along with acclimation to the new thermal regime might enhance carbon assimilation. The future carbon balance will depend on whether or not the increase in assimilation will be able to keep up with the increase in soil respiration.

Acknowledgments

The authors would like to thank M. Marushchak, V. Elsakov, R. Jensen, D. Pedersen, and I. Samarina for their contribution in field work and the Center for Permafrost (CENPERM), University of Copenhagen, for its support. This research was financially supported by the Danish Council for Independent Research | Natural Sciences (FNU) (Reference number: 645-06-0493) and the EU 6th Framework Programme Global Change and Ecosystems (CARBO-North, project contract number 036993).

References Cited

ACIA, 2005: *Arctic Climate Impact Assessment*. Cambridge and New York: Cambridge University Press, 1042 pp.

Alton, P., and Bodin, P., 2010: A comparative study of a multilayer and a productivity (light-use) efficiency land-surface model over different temporal scales. *Agricultural and Forest Meteorology*, 150: 182–195.

Aubinet, A., Grelle, A., Ibrom, A., Rannik, U., Moncrieff, J., Foken, T., Kowalski, A. S., Martin, P. H., Berbigier, P., Bernhofer, Ch., Clement, R., Elbers, J., Granier, A., Grunwald, T., Morgenstern, K., Pilegaard, K., Rebmann, C., Snijders, W., Valentini, R., and Vesala, T., 2000: Estimates of the annual net carbon and water exchange of forests: the EUROFLUX methodology. *In* Fitter, A. H., and Raffaelli, D. G. (eds.), *Advances in Ecological Research.* San Diego: Academic Press, 113–175.

Aurela, M., Laurila, T., and Tuovinen, J.-P., 2001: Seasonal CO_2 balances of a subartic mire. *Journal of Geophysical Research–Atmospheres*, 106: 1623–1637.

Baldocchi, D., 1994: A comparative study of mass and energy exchange rates over a closed C3 (wheat) and an open C4 (corn) crop: II. CO_2 exchange and water use efficiency. *Agricultural and Forest Meteorology*, 67: 291–321.

Baldocchi, D., Falge, E., Gu, L. H., Olson, R., Hollinger, D., Running, S., Anthoni, P., Bernhofer, C., Davis, K., Evans, R., Fuentes, J., Goldstein, A., Katul, G., Law, B., Lee, X. H., Malhi, Y., Meyers, T., Munger, W., Oechel, W. U. K., Pilegaard, K., Schmid, H. P., Valentini, R., Verma, S., Vesala, T., Wilson, K., and Wofsy, S., 2001: FLUXNET: a new tool to study the temporal and spatial variability of ecosystem-scale carbon dioxide, water vapor, and energy flux densities. *Bulletin of the American Meteorological Society*, 82: 2415–2434.

Baldocchi, D. D., 2003: Assessing the eddy covariance technique for evaluating carbon dioxide exchange rates of ecosystems: past, present and future. *Global Change Biology*, 9: 479–492.

Ball, J. T., Woodrow, I. E., and Berry, J. A., 1987: A model predicting stomatal conductance and its contribution to the control of photosynthesis under different environmental conditions. *In* Biggens, J. (ed.), *Progress in Photosynthesis Research.* Dordrecht: Martinus Nijhoff Publishers, 221–224.

Bewley, D., Pomeroy, J. W., and Essery, R. L. H., 2007: Solar radiation transfer through a subarctic shrub canopy. *Arctic, Antarctic, and Alpine Research*, 39: 365–374.

Bjorkman, M. P., Morgner, E., Cooper, E. J., Elberling, B., Klemedtsson, L., and Bjork, R. G., 2010: Winter carbon dioxide effluxes from arctic ecosystems: an overview and comparison of methodologies. *Global Biogeochemical Cycles*, 24: GB3010, 10 pp., http://dx.doi.org/10.1029/2009GB003667.

Bliss, L. C., and Matveyeva, N. V., 1992: Circumpolar arctic vegetation. *In* Chapin, F. S., Jefferies, R. L., Reynolds, J. F., Shaver, G. R., Svoboda, J., and Chu, E. W. (eds.), *Arctic Ecosystems in a Changing Climate: an Ecophysiological Perspective.* San Diego: Academic Press, 59–90.

Burba, G. G., McDermitt, D. K., Grelle, A., Anderson, D. J., and Xu, L. K., 2008: Addressing the influence of instrument surface heat exchange on the measurements of CO_2 flux from open-path gas analyzers. *Global Change Biology*, 14: 1854–1876.

Callaghan, T. V., Björn, L. O., Chernov, Y., Chapin, T., Christensen, T. R., Huntley, B., Ims, R. A., Johansson, M., Jolly, D., Jonasson,

S., Matveyeva, N., Panikov, N., Oechel, W., and Shaver, G., 2004: Effects on the function of arctic ecosystems in the short- and long-term perspectives. *AMBIO: A Journal of the Human Environment*, 33: 448–458.

Collatz, G. J., Ball, J. T., Grivet, C., and Berry, J. A., 1991: Physiological and environmental regulation of stomatal conductance, photosynthesis and transpiration: a model that includes a laminar boundary layer. *Agricultural and Forest Meteorology*, 54: 107–136.

Corradi, C., Kolle, O., Walter, K., Zimov, S. A., and Schulze, E. D., 2005: Carbon dioxide and methane exchange of a north-east Siberian tussock tundra. *Global Change Biology*, 11: 1910–1925.

Cox, P. M., Betts, R. A., Bunton, C. B., Essery, R. L. H., Rowntree, P. R., and Smith, J., 1999: The impact of new land surface physics on the GCM simulation of climate and climate sensitivity. *Climate Dynamics*, 15: 183–203.

Dang, Q. L., Margolis, H. A., and Collatz, G. J., 1998: Parameterization and testing of a coupled photosynthesis stomatal conductance model for boreal trees. *Tree Physiology*, 18: 141–153.

Elmendorf, S. C., Henry, G. H. R., Hollister, R. D., Björk, R. G., Bjorkman, A. D., Callaghan, T. V., Collier, L. S., Cooper, E. J., Cornelissen, J. H. C., Day, T. A., Fosaa, A. M., Gould, W. A., Grétarsdottir, J., Harte, J., Hermanutz, L., Hik, D. S., Hofgaard, A., Jarrad, F., Jónsdóttir, I. S., Keuper, F., Klanderud, K., Klein, J. A., Koh, S., Kudo, G., Lang, S. I., Loewen, V., May, J. L., Mercado, J., Michelsen, A., Molau, U., Myers-Smith, I. H., Oberbauer, S. F., Pieper, S., Post, E., Rixen, C., Robinson, C. H., Schmidt, N. M., Shaver, G. R., Stenström, A., Tolvanen, A., Totland, Ø., Troxler, T., Wahren, C. H., Webber, P. J., Welker, J. M., and Wookey, P. A., 2012: Global assessment of experimental climate warming on tundra vegetation: heterogeneity over space and time. *Ecology Letters*, 15: 164–175.

Fahnestock, J. T., Jones, M. H., and Welker, J. M., 1999: Wintertime CO_2 efflux from arctic soils: implications for annual carbon budgets. *Global Biogeochemical Cycles*, 13: 775–779.

Farquhar, G. D., Caemmerer, S., and Berry, J. A., 1980: A biochemical model of photosynthetic CO_2 assimilation in leaves of C3 species. *Planta*, 149: 78–90.

Forbes, B. C., Fauria, M. M., and Zetterberg, P., 2010: Russian arctic warming and 'greening' are closely tracked by tundra shrub willows. *Global Change Biology*, 16: 1542–1554.

Fox, A. M., Huntley, B., Lloyd, C. R., Williams, M., and Baxter, R., 2008: Net ecosystem exchange over heterogeneous arctic tundra: scaling between chamber and eddy covariance measurements. *Global Biogeochemical Cycles*, 22: GB2027, 15 pp., http://dx.doi.org/10.1029/2007GB003027.

Ghannoum, O., and Way, D. A., 2011: On the role of ecological adaptation and geographic distribution in the response of trees to climate change. *Tree Physiology*, 31: 1273–1276.

Grant, R. F., Oechel, W. C., and Ping, C. L., 2003: Modelling carbon balances of coastal arctic tundra under changing climate. *Global Change Biology*, 9: 16–36.

Groendahl, L., Friborg, T., and Soegaard, H., 2007: Temperature and snow-melt controls on interannual variability in carbon exchange in the High Arctic. *Theoretical and Applied Climatology*, 88: 111–125.

Harley, P. C., Thomas, R. B., Reynolds, J. F., and Strain, B. R., 1992: Modeling photosynthesis of cotton grown in elevated CO_2. *Plant, Cell and Environment*, 15: 271–282.

Haxeltine, A., and Prentice, I. C., 1996: A general model for the light-use efficiency of primary production. *Functional Ecology*, 10: 551–561.

Hobbie, S. E., Schimel, J. P., Trumbore, S. E., and Randerson, J. R., 2000: Controls over carbon storage and turnover in high-latitude soils. *Global Change Biology*, 6: 196–210.

IPCC, 2007: *Climate Change 2007: Working Group I: The Physical Science Basis.* Cambridge and New York: Cambridge University Press, 996 pp.

Jarvis, P. G., and McNaughton, K. G., 1986: Stomatal control of transpiration—Scaling up from leaf to region. *Advances in Ecological Research*, 15: 1–49.

Kull, O., and Jarvis, P. G., 1995: The role of nitrogen in a simple scheme to scale-up photosynthesis from leaf to canopy. *Plant Cell and Environment*, 18: 1174–1182.

Lafleur, P. M., and Humphreys, E. R., 2008: Spring warming and carbon dioxide exchange over low arctic tundra in central Canada. *Global Change Biology*, 14: 740–756.

Laurila, T., Soegaard, H., Lloyd, C. R., Aurela, M., Tuovinen, J. P., and Nordstroem, C., 2001: Seasonal variations of net CO_2 exchange in European arctic ecosystems. *Theoretical and Applied Climatology*, 70: 183–201.

Le Dizes, S., Kwiatkowski, B. L., Rastetter, E. B., Hope, A., Hobbie, J. E., Stow, D., and Daeschner, S., 2003: Modeling biogeochemical responses of tundra ecosystems to temporal and spatial variations in climate in the Kuparuk River Basin (Alaska). *Journal of Geophysical Research–Atmosphere*, 108:8165, http://dx.doi.org/10.1029/2001JD000960.

Leuning, R., 1997: Scaling to a common temperature improves the correlation between the photosynthesis parameters J_{max} and V_{cmax}. *Journal of Experimental Botany*, 48: 345–347.

Lloyd, J., and Taylor, J. A., 1994: On the temperature dependence of soil respiration. *Functional Ecology*, 8: 315–323.

Lund, M., Lafleur, P. M., Roulet, N. T., Lindroth, A., Christensen, T. R., Aurela, M., Chojnicki, B. H., Flanagan, L. B., Humphreys, E. R., Laurila, T., Oechel, W. C., Olejnik, J., Rinne, J., Schubert, P., and Nilsson, M. B., 2010: Variability in exchange of CO_2 across 12 northern peatland and tundra sites. *Global Change Biology*, 16: 2436–2448.

Marchand, F. L., Nijs, I., de Boeck, H. J., Kockelbergh, F., Mertens, S., and Beyens, L., 2004: Increased turnover but little change in the carbon balance of high-arctic tundra exposed to whole growing season warming. *Arctic, Antarctic, and Alpine Research*, 36: 298–307.

Marushchak, M. E., Kiepe, I., Biasi, C., Elsakov, V., Friborg, T., Johansson, T., Soegaard, H., Virtanen, T., and Martikainen, P. J., 2012: Carbon dioxide balance of subarctic tundra from plot to regional scales. *Biogeosciences*, Discussion, 9: 9945–9991, http://dx.doi.org/10.5194/bgd-9-9945-2012.

McFadden, J. P., Eugster, W., and Chapin, F. S., 2003: A reginoal study of the controls on water vapour and CO_2 exchange in arctic tundra. *Ecology*, 84: 2762–2776.

McGuire, A. D., Clein, J. S., Melillo, J. M, Kicklighter, D. W., Meier, R. A., Vorosmarty, C. J., and Serreze, M. C., 2000: Modeling carbon responses of tundra ecosystems to historical and projected climate: sensitivity of pan-Arctic carbon storage to temporal and spatial variation in climate. *Global Change Biology*, 6:141–159.

McGuire, A. D., Anderson, L. G., Christensen, T. R., Dallimore, S., Guo, L. D., Hayes, D. J., Heimann, M., Lorenson, T. D., Macdonald, R. W., and Roulet, N., 2009: Sensitivity of the carbon cycle in the Arctic to climate change. *Ecological Monographs*, 79: 523–555.

Miao, Z. W., Xu, M., Lathrop, R. G., and Wang, Y. F., 2009: Comparison of the A-C_c curve fitting methods in determining maximum ribulose 1.5-bisphosphate carboxylase/oxygenase carboxylation rate, potential light saturated electron transport rate and leaf dark respiration. *Plant, Cell and Environment*, 32: 109–122.

Monteith, J. L., and Unsworth, M. H., 1990: *Principles of Environmental Physics.* New York: Edward Arnold, 291 pp.

Muraoka, H., Uchida, M., Mishio, M., Nakatsubo, T., Kanda, H., and Koizumi, H., 2002: Leaf photosynthetic characteristics and net primary production of the polar willow (*Salix polaris*) in a high arctic polar semi-desert, Ny-Alesund, Svalbard. *Canadian Journal of Botany–Revue Canadienne de Botanique*, 80: 1193–1202.

Myers-Smith, I. H., Forbes, B. C., Wilmking, M., Hallinger, M., Lantz, T., Blok, D., Tape, K. D., Macias-Fauria, M., Sass-Klaassen, U., Levesque, E., Boudreau, S., Ropars, P., Hermanutz, L., Trant, A., Collier, L. S., Weijers, S., Rozema, J., Rayback, S. A., Schmidt, N. M., Schaepman-Strub, G., Wipf, S., Rixen, C., Menard, C. B., Venn, S., Goetz, S., Andreu-Hayles, L., Elmendorf, S., Ravolainen, V., Welker, J., Grogan, P., Epstein, H. E., and Hik, D. S., 2011: Shrub expansion in tundra ecosystems: dynamics, impacts and research priorities. *Environmental Research Letters*, 6: 045509, http://dx.doi.org/10.1088/1748-9326/6/4/045509.

Niu, S., Luo, Y., Fei, S., Yuan, W., Schimel, D., Law, B. E., Ammann, C., Altaf Arain, M., Arneth, A., Aubinet, M., Barr, A., Beringer, J., Bernhofer, C., Andrew Black, T., Buchmann, N., Cescatti, A., Chen,

J., Davis, K. J., Dellwik, E., Desai, A. R., Etzold, S., Francois, L., Gianelle, D., Gielen, B., Goldstein, A., Groenendijk, M., Gu, L., Hanan, N., Helfter, C., Hirano, T., Hollinger, D. Y., Jones, M. B., Kiely, G., Kolb, T. E., Kutsch, W. L., Lafleur, P., Lawrence, D. M., Li, L., Lindroth, A., Litvak, M., Loustau, D., Lund, M., Marek, M., Martin, T. A., Matteucci, G., Migliavacca, M., Montagnani, L., Moors, E., Munger, J. W., Noormets, A., Oechel, W., Olejnik, J., Kyaw, Tha Paw U, Pilegaard, K., Rambal, S., Raschi, A., Scott, R. L., Seufert, G., Spano, D., Stoy, P., Sutton, M. A., Varlagin, A., Vesala, T., Weng, E., Wohlfahrt, G., Yang, B., Zhang, Z., and Zhou, X., 2012: Thermal optimality of net ecosystem exchange of carbon dioxide and underlying mechanisms. *New Phytologist*, 194: 775–783.

Nobrega, S., and Grogan, P., 2008: Landscape and ecosystem-level controls on net carbon dioxide exchange along a natural moisture gradient in Canadian low arctic tundra. *Ecosystems*, 11: 377–396.

Oberbauer, S. F., Tweedie, C. E., Welker, J. M., Fahnestock, J. T., Henry, G. H. R., Webber, P. J., Hollister, R. D., Walker, M. D., Kuchy, A., Elmore, E., and Starr, G., 2007: Tundra CO_2 fluxes in response to experimental warming across latitudinal and moisture gradients. *Ecological Monographs*, 77: 221–238.

ORNL DAAC [Oak Ridge National Laboratory Distributed Active Archive Center], 2009: MODIS subsetted land products, Collection 5. Available from http://daac.ornl.gov/MODIS/modis.html. Oak Ridge, Tennessee: Oak Ridge National Laboratory, accessed May 2011.

Qian, H. F., Joseph, R., and Zeng, N., 2010: Enhanced terrestrial carbon uptake in the northern high latitudes in the 21st century from the coupled carbon cycle climate model intercomparison project model projections. *Global Change Biology*, 16: 641–656.

Raynolds, M. K., Comiso, J. C., Walker, D. A., and Verbyla, D., 2008: Relationship between satellite-derived land surface temperatures, arctic vegetation types, and NDVI. *Remote Sensing of Environment*, 112: 1884–1894.

Rennermalm, A. K., Soegaard, H., and Nordstroem, C., 2005: Interannual variability in carbon dioxide exchange from a high arctic fen estimated by measurements and modeling. *Arctic, Antarctic, and Alpine Research*, 37: 545–556.

Rodeghiero, M., Niinemets, U., and Cescatti, A., 2007: Major diffusion leaks of clamp-on leaf cuvettes still unaccounted: how erroneous are the estimates of Farquhar et al. model parameters? *Plant, Cell and Environment*, 30: 1006–1022.

Sage, R. F., and Kubien, D. S., 2007: The temperature response of C3 and C4 photosynthesis. *Plant, Cell and Environment*, 30: 1086–1106.

Schuur, E. A. G., Vogel, J. G., Crummer, K. G., Lee, H., Sickman, J. O., and Osterkamp, T. E., 2009: The effect of permafrost thaw on old carbon release and net carbon exchange from tundra. *Nature*, 459: 556–559.

Sellers, P. J., Berry, J. A., Collatz, G. J., Field, C. B., and Hall, F. G., 1992: Canopy reflectance, photosynthesis, and transpiration. 3. A reanalysis using improved leaf models and a new canopy integration scheme. *Remote Sensing of Environment*, 42: 187–216.

Shaver, G. R., Street, L. E., Rastetter, E. B., Van Wijk, M. T., and Williams, M., 2007: Functional convergence in regulation of net CO_2 flux in heterogeneous tundra landscapes in Alaska and Sweden. *Journal of Ecology*, 95: 802–817.

Sitch, S., Smith, B., Prentice, I. C., Arneth, A., Bondeau, A., Cramer, W., Kaplan, J. O., Levis, S., Lucht, W., Sykes, M. T., Thonicke, K., and Venevsky, S., 2003: Evaluation of ecosystem dynamics, plant geography and terrestrial carbon cycling in the LPJ dynamic global vegetation model. *Global Change Biology*, 9: 161–185.

Sitch, S., McGuire, A. D., Kimball, J., Gedney, N., Gamon, J., Engstrom, R., Wolf, A., Zhuang, Q., Clein, J., and McDonald, K. C., 2007: Assessing the carbon balance of circumpolar arctic tundra using remote sensing and process modeling. *Ecological Applications*, 17: 213–234.

Soegaard, H., and Nordstroem, C., 1999: Carbon dioxide exchange in a high-arctic fen estimated by eddy covariance measurements and modelling. *Global Change Biology*, 5: 547–562.

Soegaard, H., Nordstroem, C., Friborg, T., Hansen, B. U., Christensen, T. R., and Bay, C., 2000: Trace gas exchange in a high-arctic valley 3. Integrating and scaling CO_2 fluxes from canopy to landscape using flux data, footprint modeling, and remote sensing. *Global Biogeochemical Cycles*, 14: 725–744.

Sturm, M., McFadden, J. P., Liston, G. E., Chapin, F. S., Racine, C. H., and Holmgren, J., 2001: Snow-shrub interactions in arctic tundra: a hypothesis with climatic implications. *Journal of Climate*, 14: 336–344.

Tarnocai, C., Canadell J. G., Schuur, E. A. G., Kuhry, P., Mazhitova, G., and Zimov, S., 2009: Soil organic carbon pools in the northern circumpolar permafrost region. *Global Biogeochemical Cycles*, 23: GB2023, 11 pp., http://dx.doi.org/10.1029/2008GB003327.

Thum, T., Aalto, T., Laurila, T., Aurela, M., Lindroth, A., and Vesala, T., 2008: Assessing seasonality of biochemical CO_2 exchange model parameters from micrometeorological flux observations at boreal coniferous forest. *Biogeosciences*, 5: 1625–1639.

Verbyla, D. L., 2005: Assessment of the MODIS leaf area index product (MOD15) in Alaska. *International Journal of Remote Sensing*, 26: 1277–1284.

Vogel, J., Schuur, E. A. G., Trucco, C., and Lee, H., 2009: Response of CO_2 exchange in a tussock tundra ecosystem to permafrost thaw and thermokarst development. *Journal of Geophysical Research–Biogeosciences*, 114: G04018, 14 pp., http://dx.doi.org/10.1029/2008JG000901.

Vourlitis, G. L., Oechel, W. C., Hope, A., Stow, D., Boynton, B., Verfaillie, J., Zulueta, R., and Hastings, S. J., 2000: Physiological models for scaling plot measurements of CO_2 flux across an arctic tundra landscape. *Ecological Applications*, 10: 60–72.

Walker, M. D., Wahren, C. H., Hollister, R. D., Henry, G. H. R., Ahlquist, L. E., Alatalo, J. M., Bret-Harte, M. S., Calef, M. P., Callaghan, T. V., Carroll, A. B., Epstein, H. E., Jonsdottir, I. S., Klein, J. A., Magnusson, B., Molau, U., Oberbauer, S. F., Rewa, S. P., Robinson, C. H., Shaver, G. R., Suding, K. N., Thompson, C. C., Tolvanen, A., Totland, O., Turner, P. L., Tweedie, C. E., Webber, P. J., and Wookey, P. A., 2006: Plant community responses to experimental warming across the tundra biome. *Proceedings of the National Academy of Sciences of the United States of America*, 103: 1342–1346.

Welker, J. M., Fahnestock, J. T., Henry, G. H. R., O'Dea, K. W., and Chimner, R. A., 2004: CO_2 exchange in three Canadian high arctic ecosystems: response to long-term experimental warming. *Global Change Biology*, 10: 1981–1995, http://dx.doi.org/10.1111/j.1365-2486.2004.00857.x.

Williams, M., Rastetter, E. B., Fernandes, D. N., Goulden, M. L., Wofsy, S. C., Shaver, G. R., Melillo, J. M., Munger, J. W., Fan, S. M., and Nadelhoffer, K. J., 1996: Modelling the soil-plant-atmosphere continuum in a *Quercus Acer* stand at Harvard Forest: the regulation of stomatal conductance by light, nitrogen and soil/plant hydraulic properties. *Plant, Cell and Environment*, 19: 911–927.

Williams, M., Eugster, W., Rastetter, E. B., McFadden, J. P., and Chapin, F. S., 2000: The controls on net ecosystem productivity along an arctic transect: a model comparison with flux measurements. *Global Change Biology*, 6: 116–126.

Williams, M., Street, L. E., Van Wijk, M. T., and Shaver, G. R., 2006: Identifying differences in carbon exchange among arctic ecosystem types. *Ecosystems*, 9: 288–304.

Wullschleger, S. D., 1993: Biochemical limitations to carbon assimilation in C3 Plants—A retrospective analysis of the A/C_i curves from 109 species. *Journal of Experimental Botany*, 44: 907–920.

Zamolodchikov, D. G., and Karelin, D. V., 2001: An empirical model of carbon fluxes in Russian tundra. *Global Change Biology*, 7: 147–161.

MS accepted August 2012